OPEN ACCESS Freely available online

PLoS one

An Electronic Analog of Synthetic Genetic Networks

Edward H. Hellen[1]*, Evgenii Volkov[2], Jurgen Kurths[3], Syamal Kumar Dana[4]

1 Department of Physics and Astronomy, University of North Carolina Greensboro, Greensboro, North Carolina, United States of America, **2** Department of Theoretical Physics, Lebedev Physical Institute, Moscow, Russia, **3** Potsdam Institute for Climate Impact Research, Potsdam, Germany, **4** Indian Institute of Chemical Biology, Council of Scientific and Industrial Research, Kolkata, India

Abstract

An electronic analog of a synthetic genetic network known as the *repressilator* is proposed. The *repressilator* is a synthetic biological clock consisting of a cyclic inhibitory network of three negative regulatory genes which produces oscillations in the expressed protein concentrations. Compared to previous circuit analogs of the *repressilator*, the circuit here takes into account more accurately the kinetics of gene expression, inhibition, and protein degradation. A good agreement between circuit measurements and numerical prediction is observed. The circuit allows for easy control of the kinetic parameters thereby aiding investigations of large varieties of potential dynamics.

Citation: Hellen EH, Volkov E, Kurths J, Dana SK (2011) An Electronic Analog of Synthetic Genetic Networks. PLoS ONE 6(8): e23286. doi:10.1371/journal.pone.0023286

Editor: Matjaz Perc, University of Maribor, Slovenia

Received June 26, 2011; **Accepted** July 12, 2011; **Published** August 4, 2011

Funding: Travel funds to EHH were provided by the International Programs Center at the University of North Carolina Greensboro. The funders had no role in study design, data collection and analysis, decision to publish, or preparation of the manuscript.

Competing Interests: The authors have declared that no competing interests exist.

* E-mail: ehhellen@uncg.edu

Introduction

The concept of synthesizing simple gene units to realize a desired function or to reproduce a known function is new [1] in biological systems. After confirmation of the unit's desired functional behavior, a large assembly of such units can be organized to perform complex biological functions [2–4]. This is like engineering small integrated chips to build a computer to derive a targeted function. In efforts towards engineering biological functions, a *repressilator* was first demonstrated as a synthetic genetic clock expressed in *Escherchia coli* [5] producing oscillations in expressed protein concentrations. A mathematical model based on standard chemical kinetics was also proposed that predicted the observed oscillations.

The dynamics of coupled synthetic genetic networks (SGNs) was also investigated [6–7] theoretically to understand the generation of synchronous rhythm in an assembly of *repressilator*s via quorum sensing type interaction. Quorum sensing [8] is a form of exchanging information that a bacterial colony uses to develop a common rhythm. This quorum sensing type of indirect coupling is set-up between the SGN cells through diffusion of auto-inducing small molecules in a common medium. When the feedback via auto-inducing agents inside a SGN cell is reinforcing [7], the coupled dynamics show a state of in-phase synchrony, whereas when the feedback is repulsive, then the coupled dynamics show various possible states [9–11]: in-phase and anti-phase synchrony, inhomogeneous limit cycles, inhomogeneous steady states, and homogeneous steady states. Recently, in a biological experiment [12], evidence of in-phase synchronized quorum of genetic clock units was found. However, more complex features, as chaos, antiphase, and multistability in synchronous rhythm of coupled genetic clocks are yet to be observed experimentally.

Mathematical models are always a very useful tool to predict complex behaviors of dynamical systems using numerical simulations. Experimental verification of rich multistability requires an accurate knowledge of the model parameters which is often very challenging in biological experiments. An alternative experimental approach using electronic analogs of the SGN was undertaken [13–15] to confirm the numerical results and to search for possible coupled dynamics. Although it is difficult to simulate the biological experiment exactly in a circuit, the advantage of an electronic SGN is accessibility of system parameters and their controllability that allows a systematic exploration of known and predictable dynamics. Earlier [13–15] electronic circuit analogs of SGN displayed oscillations with 120° phase shifts between the oscillating variables, qualitatively in agreement with the genetic *repressilator*, however, the multistability of coupled SGNs was missing since access to and control of the system parameters was lacking.

In this paper, an electronic analog of the SGN is specifically designed to derive more accurate kinetic parameters of the *repressilator*. The goal is to control the parameters and thereby to realize desired sets of various kinetic parameters used in the simulations of the mathematical model. As a result, the circuit shows agreement between the measurements and the numerical predictions. The building block for the electronic *repressilator* is a circuit model for a single negative regulatory gene. This circuit shall be useful in a variety of other SGN investigations in addition to the *repressilator*. Designing electronic circuits of SGN also has the purpose of reverse engineering where knowledge of the biological experiments can be utilized for new technology and applications [16].

Methods

Genetic Network Repressilator

The structure of the *repressilator* consists of three repressive genes connected in a loop [5], with each gene producing repressor to the subsequent gene. The genes ($i = 1,2,3$) each produce their own mRNA, which translate the repressor protein. Gene 1′s repressor inhibits transcription of gene 2′s mRNA, 2′s repressor inhibits 3′s mRNA, and 3′s repressor inhibits 1′s mRNA. Taking into account

standard chemical kinetics for production, degradation and inhibition, a dynamical system model of 6 first order differential equations was used for the mRNA and the protein concentrations [5].

An electronic analog of the *repressilator* was also proposed earlier [14–15], where they used three voltages as the variables, thus reducing the above model to a set of three differential equations. However, these circuits did not simulate the kinetic parameters of the *repressilator* model. A reduced three variable model is also used here but special care is taken to retain the parameters for the chemical kinetics as in the original model [5]. The reduced genetic network (RGN) *repressilator* is defined as,

$$\dot{x}_i = \beta_i\left(-x_i + \frac{\alpha}{1+x_{i-1}^n}\right) \tag{1}$$

where $i = 1, 2, 3$ for three genes, and the loop is closed by the condition $x_0 = x_3$. The product of the i^{th} gene is x_i, and its production is inhibited by x_{i-1}. The parameter α accounts for the maximum transcription rate in the absence of an inhibitor, β is the decay rate of protein degradation and n is the Hill coefficient for inhibition. The Hill function is commonly used to account for sigmoidal binding kinetics. In this RGN model, there is no distinction between the mRNA and the transcribed repressor protein. We find that by this reduction, the fundamental features of the SGN model are not affected.

Description of the RGN Circuit

The building block for the RGN *repressilator* circuit is the circuit for a single negative regulatory gene shown in Fig. 1. The desired dynamics are given by (1), where x_i corresponds to the output of the circuit and x_{i-1} is the input. The goal is to use a circuit which accounts for the kinetics of gene inhibition, production of repressor, and degradation of repressor. The gene's product is analogous to the charge coming from the collector of the transistor and the rate of production is the transistor current. The concentration of product x_i is proportional to the voltage V_i across the capacitor, and the rate of decay is the current through R_C. The kinetics of gene inhibition is determined by the circuitry that couples the input voltage V_{i-1} (the inhibitor) to the voltage at the base of the transistor.

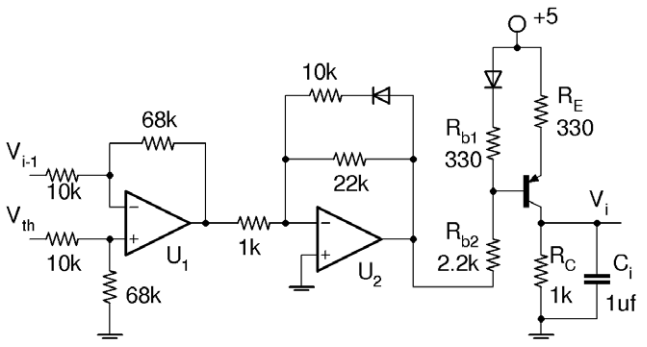

Figure 1. Electronic circuit analog of negative regulatory gene. V_{i-1} at the input is the concentration of inhibitory repressor. The circuit output V_i is the concentration of the gene's product. V_{th} accounts for the binding constant of the repressor to the gene's DNA. As inhibitor concentration V_{i-1} increases past V_{th}, the voltage at the transistor base rises, turning the transistor's collector current off, thereby stopping gene production. Op-amps are LF412, diodes are 1N4148, *pnp* transistor is 2N3906, and +/−5 V supply.
doi:10.1371/journal.pone.0023286.g001

Circuit Analysis. Here the circuit parameters are determined that correspond to particular values of kinetic parameters α, β_i, and n in (1). The dynamical equation for voltage V_i is

$$\frac{dV_i}{dt} = \frac{1}{R_C C_i}\left(-V_i + R_C I_t(V_{i-1})\right) \tag{2}$$

where $I_t(V_{i-1})$ is the transistor's collector current and V_{i-1} is the variable input voltage. The equations are expressed in dimensionless form using dimensionless time t/τ where the time-scale is chosen by $\tau = R_C C_0$. The capacitor value is then $C_i = C_0/\beta_i$ and (2) becomes

$$\dot{V}_i = \beta_i\left(-V_i + R_C I_t(V_{i-1})\right) \tag{3}$$

where the dot denotes time derivative in dimensionless time τ. In order for the circuit to model the gene kinetics it is desired that $I_t(V_{i-1})$ approximates the Hill function,

$$I_t(V_{i-1}) \approx \frac{I_{\max}(V_{th})^n}{(V_{th})^n + (V_{i-1})^n} = \frac{I_{\max}}{1+(x_{i-1})^n} \tag{4}$$

where $x_{i-1} = V_{i-1}/V_{th}$ and V_{th} represents an equilibrium constant for binding of repressor x_{i-1} to the gene's DNA. $I_{\max}$ is the maximum current through the transistor corresponding to gene transcription in the absence of an inhibitor. The production is half-maximal, $I_t = I_{\max}/2$, when $V_{i-1} = V_{th}$. Dividing both sides of (3) by V_{th}, the α and β_i are given by $\alpha = I_{\max}R_C/V_{th}$ and $\beta_i = C_0/C_i$. Note that $I_{\max}$ is not due to saturation of the transistor since the voltage $I_{\max}R_C$ is chosen so that the emitter-collector voltage across the transistor does not reach zero. Instead $I_{\max}$ is due to saturation of the op-amp as discussed below.

Next we determine how the Hill coefficient n relates to the circuit parameters. The Hill function behavior consists of a transition of V_i from one value to another one as V_{i-1} increases, with the transition occurring in the region around $V_{i-1} = V_{th}$ as shown in Fig. 2. In addition the slope in the transition region is not

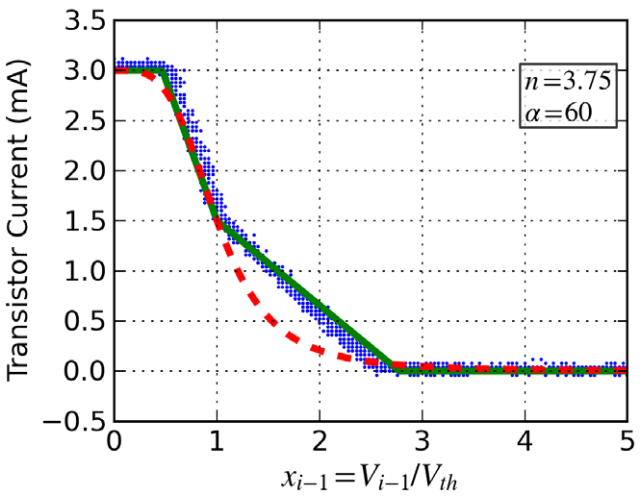

Figure 2. Hill function inhibitory response. Hill function inhibition of gene expression is approximated by the transistor current's dependence on input voltage V_{i-1} for the circuit in Fig. 1. Hill function (red dashed line), predicted current (green solid line), and measured current (blue dots). Maximum transistor current of 3 mA corresponds to maximum transcription rate $\alpha = 60$. The Hill coefficient is $n = 3.75$.
doi:10.1371/journal.pone.0023286.g002

constant. The circuit using the two op-amps U_1 and U_2 approximates this behavior by saturating the op-amp output and by using different gains in the transition region, a larger gain for $V_{i\text{-}1} < V_{th}$ and smaller for $V_{i\text{-}1} > V_{th}$. Op-amp U_1 is configured as a subtraction amplifier with output $G_1(V_{\text{i-1}} - V_{\text{th}}) = G_1\Delta V$ where G_1 is negative. Op-amp U_2 has different gains G_{+2} and G_{-2} depending on the sign of ΔV. Taking saturation of the outputs into account gives the voltage at the output of U_2,

$$G\Delta V = \begin{cases} V_{+sat} & G_1G_{+2}\Delta V > V_{+sat} \\ G_1G_{+2}\Delta V & 0 < G_1G_{+2}\Delta V < V_{+sat} \\ G_1G_{-2}\Delta V & V_{-sat} < G_1G_{-2}\Delta V < 0 \\ V_{-sat} & G_1G_{-2}\Delta V < V_{-sat} \end{cases} \quad (5)$$

where $V_{\pm sat}$ are the saturation levels.

The next step is to consider how $G\Delta V$ controls the transistor current. The voltage drop across R_{b1} is

$$V_{Rb1} = \frac{R_{b1}}{R_{b1}+R_{b2}}(V_{CC} - 0.6 - G\Delta V) \quad (6)$$

where the forward bias voltage drop across the diode is 0.6 V and V_{CC} is the supply voltage, +5 V. The diode in series with R_{b1} compensates for the transistor's emitter-base voltage drop, so that the voltage across R_{b1} is approximately the same as the voltage across R_{E}. The current $I_t(V_{\text{i-1}})$ through R_{E} and the transistor is therefore (6) divided by R_{E}. The maximum current $I_{\max}$ occurs when the output of U_2 is saturated at $G\Delta V = V_{-sat}$, giving

$$I_{\max} = \frac{R_{b1}}{R_{b1}+R_{b2}}\frac{(V_{CC} - 0.6 - V_{-sat})}{R_E}. \quad (7)$$

For comparison with the Hill function it is useful to express I_t in terms of I_{max} and the normalized input voltage $x_{\text{i-1}}$,

$$I_t(x_{i-1}) = \frac{I_{\max}V_{th}}{(V_{CC} - 0.6 - V_{-sat})}\left(\frac{V_{CC} - 0.6}{V_{th}} - G\Delta x_{i-1}\right) \quad (8)$$

where $\Delta x_{i\text{-}1} = (x_{\text{i-1}} - 1)$.

In order to approximate the Hill function the overall gain G_1G_{-2} for $V_{\text{i-1}} < V_{th}$ is chosen such that slope $dI_t/dx_{\text{i-1}}$ of the transistor current matches the slope of the Hill function at $x_{\text{i-1}} = 1$ ($V_{\text{i-1}} = V_{\text{th}}$). At $x_{\text{i-1}} = 1$, the output $G\Delta V$ is not saturated, so $G = G_1G_{-2}$. Equating the slopes gives the condition relating Hill coefficient n to the overall gain G_1G_{-2},

$$n = 4G_1G_{-2}V_{th}/(V_{CC} - 0.6 - V_{-sat}). \quad (9)$$

Choosing the gain G_{+2} (for $V_{\text{i-1}} > V_{th}$) to be less than G_{-2} improves the transistor current's approximation to the Hill function. We find that choosing $G_{+2} \cong 0.3G_{-2}$ works well for a range of parameter values α, β_i, and n. Fig. 2 shows the Hill function (red dashed) and the predicted (green solid) and measured (blue dots) transistor current for $n = 3.75$.

Model Parameters, Circuit Parameters, and Design Considerations. Given a circuit it is useful to be able to easily determine the corresponding model parameters. From the previous section α, β_i, and n, are expressed in terms of circuit parameters by

$$\alpha = I_{\max}R_C/V_{th} \quad (10)$$

$$\beta_i = C_0/C_i \quad (11)$$

$$n = 4G_1G_{-2}V_{th}/(V_{CC} - 0.6 - V_{-sat}). \quad (12)$$

As an example, in Fig. 1 the gain for op-amp U_1 is $G_1 = -6.8$ and gain for op-amp U_2 is $G_{-2} = -22$ for non-saturated overall gain $G_1G_{-2} = 150$. For $V_{\text{i-1}} > V_{\text{th}}$ the gain G_{+2} is approximately -6.9. For $V_{\text{th}} = 50$ mV, $C_0 = 1$ µf, $I_{\max} = 3$ mA, supply $V_{CC} = 5$ V, and LF412 op-amp saturation $V_{-sat} = -3.5$ V, the resulting model parameters are $\alpha = 60$, $\beta_i = 1$, and $n = 3.8$.

It is also useful to be able to determine circuit parameters that achieve a desired set of model parameters. Starting with (10), $I_{\max}R_C$ must be far enough below the supply V_{CC} so that the emitter-collector voltage of the transistor never reaches zero. For $V_{\text{CC}} = 5$ V, $I_{\max}R_C$ is chosen to be around 3 volts and the emitter-collector voltage never gets less than about 1volt so that the transistor never goes into saturation. The choice of $I_{\max}$ has some freedom. For $I_{\max} = 3$ mA, this determines $R_C = 1$ kΩ and $R_E = 330$ Ω in order to get voltage drops of 1, 1, and 3 volts across R_E, the transistor, and R_C, respectively, when $I_{\text{t}} = I_{\max}$. The remaining free circuit parameter to adjust for a desired value of α is V_{th}. Rearranging (10) gives

$$V_{th} = I_{\max}R_C/\alpha. \quad (13)$$

For example, for $I_{\max}R_C = 3$ V, a value of $\alpha = 100$ is obtained using $V_{\text{th}} \cong 30$ mV. The capacitor value C_{i} to use for a desired β_i is easily given by (11) as

$$C_i = C_0/\beta_i. \quad (14)$$

The third circuit parameter is the overall gain G_1G_{-2} which is determined by n and α. Rearranging (12) gives

$$G_1G_{-2} = \frac{(V_{CC} - 0.6 - V_{-sat})n}{4V_{th}} = \frac{V_{CC} - 0.6 - V_{-sat}}{4I_{\max}R_C}n\alpha. \quad (15)$$

For $V_{CC} = 5$ V and $V_{-sat} = -3.5$ V, then $V_{CC} - 0.6 - V_{-sat} = 7.9$ V, and with $I_{\max}R_C = 3$ V, then $G_1G_{-2} \approx 2n\alpha/3$. For example, if the desired parameter values are $\alpha = 100$ and $n = 4$, then the required overall gain is $G_1G_{-2} \approx 267$ which can be split as desired between G_1 and G_{-2}. Thus, the circuit parameters that are adjusted to obtain a desired set of model parameters are V_{th}, C_{i}, and G_1G_{-2}.

A careful selection of the op-amp is important for good approximation of the Hill function by the transistor current. The op-amp must be able to recover satisfactorily from saturation of its output. The circuit in Fig. 1 is tested with V_{th} set to zero and with $C_i = 0$. Results for the LF412 are shown in Fig. 3. The input voltage $V_{\text{i-1}}$ (blue line) is a triangle wave from a signal generator and the measured outputs are $G\Delta V$ (red line) from the output of U_2 and the final output voltage V_{i} (green line). The red curve shows that the LF412 saturates at $V_{+sat} = +4.5$ V and at $V_{-sat} = -3.5$ V when using a ±5 V supply, and that the circuit makes the

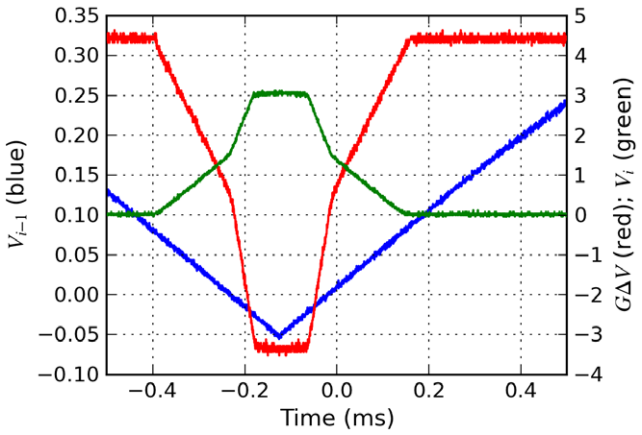

Figure 3. Measured time response of single gene circuit. Time response for the single gene circuit in Fig. 1 with $V_{th} = 0$ and $C_i = 0$. Input $V_{i\text{-}1}$ (blue), op-amp output $G\Delta V$ (red), final output V_i (green). The red curve shows saturation of the op-amp output at +4.5 and –3.5 V when using a +/–5 V supply. The change in slope when $V_{i\text{-}1} = V_{th}$ is also apparent.
doi:10.1371/journal.pone.0023286.g003

transition from high gain to low gain when $V_{i\text{-}1}$ goes from negative to positive corresponding to $x_{i\text{-}1}$ surpassing one. The green line shows the expected inhibitory response with respect to input $V_{i\text{-}1}$, and the maximum value of $I_{max}R_C = 3$ V.

***Repressilator* Circuit.** The electronic *repressilator* circuit consists of three negative regulatory gene circuits (Fig. 1) connected in an inhibitory loop as shown in Fig. 4. The triangle symbol contains the 2 op-amps, transistor, and circuitry which determine parameters α and n.

Results and Discussion

The model parameters α, β_i, and n are now ably determined by circuit parameters. Our results of circuit measurements and numerical predictions are shown for three cases: (1) identical genes, β-ratio = 1:1:1; (2) gene $i = 1$ with faster decay, β-ratio = 3:1:1; (3) gene $i = 1$ with slower decay, β-ratio = 0.3:1:1. Gene products are the normalized voltages x_1 (blue), x_2 (red), and x_3 (green). Circuit measurements are solid lines, numerical predictions are dashed lines. The circuit parameters V_{th} and overall gain G_1G_2 were varied using (13) and (15) in order to set α and n. V_{th} varied from 30 mV to 120 mV, and G_1G_2 from 73 to 220 corresponding to $\alpha = 25$ to 100 and $n = 3.0$ to 6.6. The figures show results for $(\alpha, n) = (50, 6.6)$ and (100, 3.3). Other sets of parameters produced results with similar agreement of measurements and numerical predictions. The time constant was $\tau = R_CC_0 = (1\ k\Omega)(1\ \mu f) = 1$ ms. It follows that $C_i = (1\ \mu f)/\beta_i$.

Fig. 5 shows the *repressilator* dynamics for β-ratio = 1:1:1 where $C_i = 1$ µf for each capacitor. The three state variables have the same shape, but with 120° phase shift. Numerical predictions are in close agreement with the measurements.

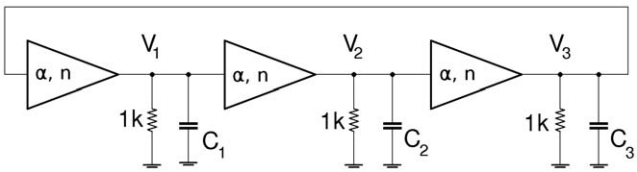

Figure 4. Electronic repressilator. Repressilator circuit constructed from a loop of three of the negative regulatory gene circuits of Fig. 1.
doi:10.1371/journal.pone.0023286.g004

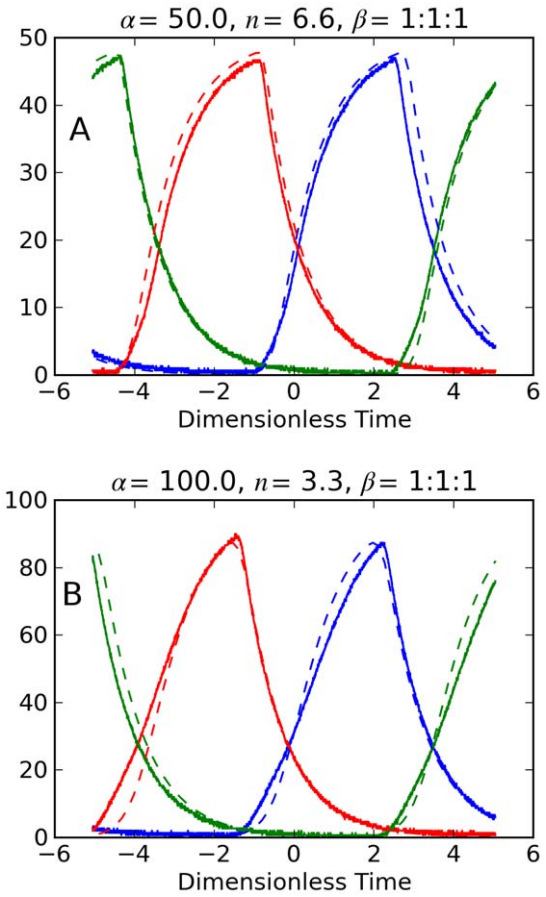

Figure 5. Electronic repressilator dynamics. Normalized voltages x_i measured from RGN repressilator circuit (solid) and numerical predictions (dashed). β-ratio = 1:1:1. Panel A ($\alpha = 50$, $n = 6.6$); Panel B ($\alpha = 100$, $n = 3.3$).
doi:10.1371/journal.pone.0023286.g005

For the dynamics in Fig. 6 gene $i = 1$ has its capacitor reduced to 0.33 µf, so it has $\beta_1 = 3$. Thus the β -ratio for the genes in the *repressilator* circuit is 3:1:1. Increasing the gene product's decay rate causes larger oscillations for the product, reduced oscillations for the gene's inhibitor, and an increased oscillation frequency for the *repressilator*.

For the dynamics in Fig. 7 electronic gene $i = 1$ has its capacitor increased to 3.3 µf, so it has $\beta_1 = 0.3$. Thus the β-ratio for the genes in the *repressilator* circuit is 0.3:1:1. Gene $i = 1$ now has reduced oscillations, its inhibitor gene $i = 3$ has increased oscillations, and the *repressilator* frequency has decreased.

The circuit presented here as an electronic analog of a synthetic genetic network known as the *repressilator* shows good agreement between experimental measurements and numerical predictions. The circuit includes control of parameters for the Hill function which is used to model the kinetics of gene expression and inhibition in the cyclic 3-gene network. Previous electronic analogs of the *repressilator* [14–15] did not concentrate on the kinetics and control of the parameters, and thereby did not capture many complex dynamical features. With the ability to control the model parameters, this circuit will be useful for investigations of multistability of coupled *repressilators* as well as for other SGN dynamics.

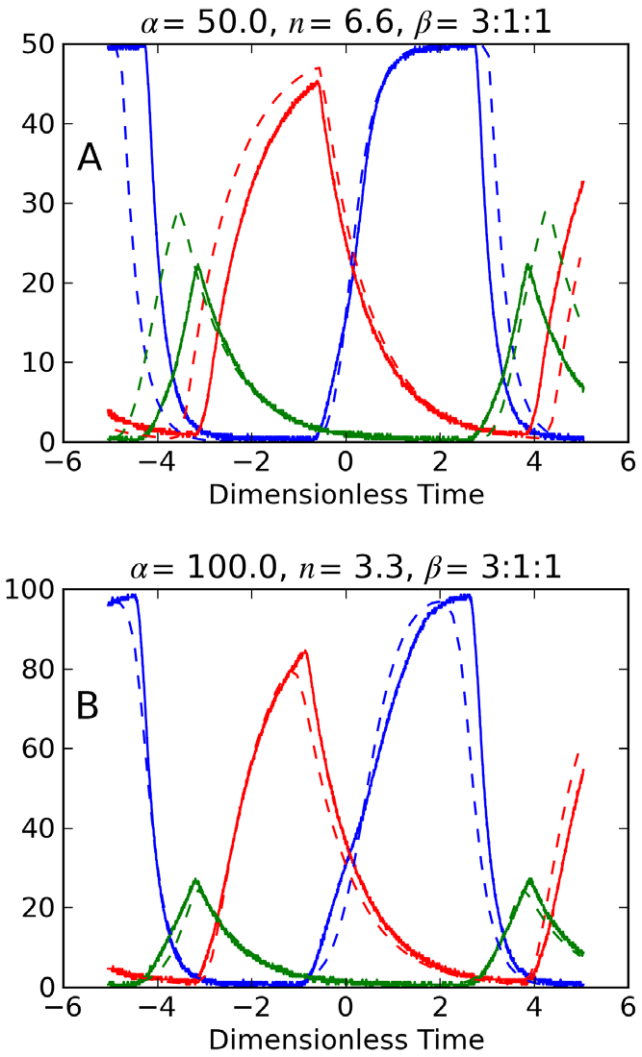

Figure 6. Electronic repressilator dynamics with one fast decay rate. Normalized voltages x_i measured from RGN repressilator circuit (solid) and numerical predictions (dashed). β-ratio = 3:1:1. Panel A ($\alpha = 50$, $n = 6.6$); Panel B ($\alpha = 100$, $n = 3.3$).
doi:10.1371/journal.pone.0023286.g006

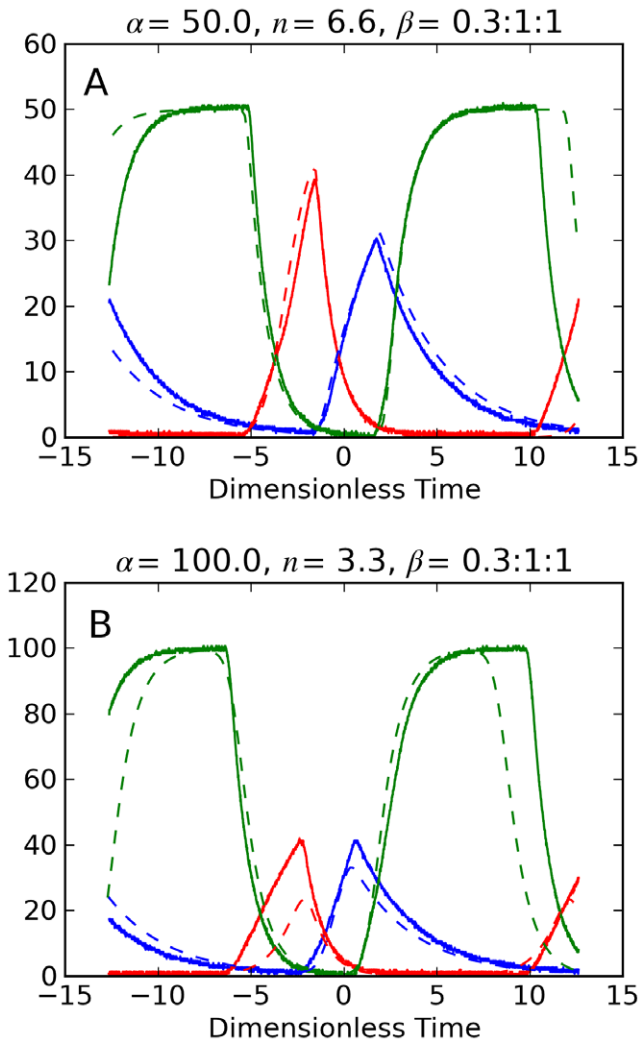

Figure 7. Electronic repressilator dynamics with one slow decay rate. Normalized voltages x_i measured from RGN repressilator circuit (solid) and numerical predictions (dashed). β-ratio = 0.3:1:1. Panel A ($\alpha = 50$, $n = 6.6$); Panel B ($\alpha = 100$, $n = 3.3$).
doi:10.1371/journal.pone.0023286.g007

Acknowledgments

The authors thank Siddhartha Roy, Indian Institute of Chemical Biology, for valuable comments and suggestions.

Author Contributions

Conceived and designed the experiments: EHH EV JK SKD. Performed the experiments: EHH. Analyzed the data: EHH SKD. Wrote the paper: EHH SKD.

References

1. Elowitz M, Lim WA (2010) Build life to understand it. Nature 468: 889–890.
2. Gardner TS, Cantor CR, Collins JJ (2000) Construction of a genetic toggle switch in *Escherichia Coli*. Nature (London) 403: 339–342.
3. You L, Cox RS, Weiss R, Arnold FH (2004) Programmed population control by cell-cell communication and regulated killing. Nature 428: 868–871.
4. Bell-Pederson D, Cassone VM, Earnest DJ, Golden SS, Hardin PE, et al. (2005) Circadian rhythms from multiple oscillators: lessons from diverse organisms. Nat Rev Genet 6: 544–556.
5. Elowitz MB, Leibler S (2000) A synthetic oscillatory network of transcriptional regulators. Nature 403: 335–338.
6. Yamaguchi S, Isejima H, Matsuo T, Okura R, Yagita K, et al. (2003) Synchronization of cellular clocks in the suprachiasmatic nucleus. Science 302: 1408–1412.
7. García-Ojalvo J, Elowitz M, Strogatz SH (2004) Modelling a synthetic multicellular clock: repressilators coupled by quorum sensing. Proc Nat Acad Sci 101: 10955–10960.
8. Lerat E, Moran NA (2004) Evolutionary history of quorum-sensing systems in bacteria. Molecular Biology and Evolution 21: 903–913.
9. Ullner E, Zaikin A, Volkov EI, García-Ojalvo J (2007) Multistability and clustering in a population of synthetic genetic oscillators via phase-repulsive cell-to-cell communication. Phy Rev Lett 99: 148103.
10. Ullner E, Koseska A, Kurths J, Volkov EI, Kantz H, et al. (2008) Multistability of synthetic genetic networks with repressive cell-to-cell communication. Phy Rev E 78: 031904.
11. Potapov I, Volkov E, Kuznetsov A (2011) Dynamics of coupled repressilators: The role of mRNA kinetics and Transcription cooperativity. Phy Rev E 83: 031901.
12. Danino T, Mondragón-Palomino O, Tsimring L, Hasty J (2010) A Synchronized quorum of genetic clocks. Nature 463: 326–330.
13. Mason J, Linsay PS, Collins JJ, Glass L (2004) Evolving complex dynamics in electronic models of genetic networks. Chaos 14: 707–715.
14. Wagemakers A, Buldú JM, García-Ojalvo J, Sanjuán MAF (2006) Synchronization of electronic genetic networks. Chaos 16: 013127.
15. Buldú JM, García-Ojalvo J, Wagemakers A, Sanjuán MAF (2007) Electronic design of synthetic genetic networks. Int J Bifur Chaos 17: 3507–3511.
16. Lucks JB, Arkin AP (2011) The hunt for the biological transistor: How genetic circuits will unlock the true potential of bioengineering. IEEE Spectrum 48: 34–39.